JBAT 12(1) (2023) 52 – 62

Jurnal Bahan Alam Terbarukan

Accredited SINTA 2 by Ministry of Research and Technology/National Research and Innovation Agency
SK No. 200/M/KPT/2020
http://journal.unnes.ac.id/nju/index.php/jbat

p-ISSN 2303 0623
e-ISSN 2407 2370

Effects of Steam-To-Biomass Ratio and Temperature in Gasification on The Methanol Conversion and Selectivity: A Simulation Study of Biomass to Methanol

Rahma Muthia[1,2,✉], Muhammad Raihan Pratama[1,2]

DOI: https://doi.org/10.15294/jbat.v12i1.42365

[1] Chemical Engineering Department, Faculty of Engineering, Universitas Indonesia, Depok 16424, Indonesia
[2] Sustainable Energy Systems and Policy Research Cluster, Universitas Indonesia, Depok, 16424, Indonesia

Article Info

Article history:
Received
18 January 2023
Revised
15 March 2023
Accepted
31 March 2023
Online
12 May 2023

Keywords:
Gasification temperature;
Methanol;
Simulation;
Steam gasification;
Steam-to-biomass ratio

Abstract

Gasification is an attractive pathway for valorizing waste and biomass as it can deal with a wide range of feedstocks yielding gaseous products that be converted further to valuable biofuels and chemicals. While many previous studies commonly discussed the effects of gasification operating parameters, such as operating conditions, biomass feedstocks and gasifying agents, on syngas compositions, fewer studies evaluated the effects of gasification process parameters on final products derived from syngas. Essentially, performing an integrated assessment of the biomass-to-product conversion gives a thorough understanding of the biomass processing and provides one with useful heuristics for the conversion of biomass to valuable chemicals. This study evaluates the effects of steam-to-biomass ratio (S/B = 0.3 – 0.7) and gasification temperature (T_{gasif} = 900°C – 1,100°C) on the methanol production by performing simulations in the Aspen Plus v.11 process simulator. The kinetically controlled reactions model was considered in the methanol synthesis unit to mimic its actual process condition and to take into account the possibility of the side product formation. The outcome of this study recommends that the steam-to-biomass ratio gives more notable effects on the gasification distribution products and the conversion of syngas to methanol than those given by the gasification temperature. While, the reaction selectivity to methanol remains high, and it is not sensitive to the change of steam-to-biomass ratios and gasification temperatures.

INTRODUCTION

The industrial and scientific societies across the world aim for establishing technologies and methods to produce and utilize sustainable fuels and chemicals in the way of reducing the reliance on fossil fuels. Biomass is an attractive raw material for many bio-based products as it is considered to be CO_2 neutral. It is abundantly available in different regions in the forms of agricultural and forestry residue, crops, and wastes, e.g., municipal solid and sewage waste. Biomass contains significant amounts of polysaccharides and lignin that can be converted to monomer sugars and further valorized for the production of high value-added biochemicals (Vu et al., 2020).

The conversion of biomass to energy and chemicals may occur via thermochemical, biochemical or hybrid processes (Marulanda et al., 2019). In general, thermochemical processes offer higher efficiencies over biochemical processes as they require shorter reaction time and they have superior ability in decomposing most of organic compounds, such as lignin (Zhang et al., 2010). Thermochemical conversion processes of biomass consist of direct combustion, gasification, pyrolysis and thermal liquefaction. Among those processes, gasification yields gases, which are mainly carbon monoxide, carbon dioxide, hydrogen and methane,

✉ Corresponding author:
E-mail: rahmamuthia@ui.ac.id

that be converted further to valuable biofuels and chemicals via either catalytic conversion or anaerobic fermentation (Xiong et al., 2017; You et al., 2018).

Overviews of gasification technology are widely available in literature (Panwar et al., 2012; Molino et al., 2018; Marulanda et al., 2019; Mutlu et al., 2020). Previous studies simulated the conversion of biomass to syngas by considering different reactor configurations. For example, Begum et al. (2014) developed a numerical approach for optimizing gasification conditions in a fluidized bed reactor. Gao et al. (2016) established an intrinsic reaction rate sub-model based on the Euler-Lagrange method for biomass gasification in an entrainer flow gasifier. Fajimi et al. (2021) performed simulation studies using the Aspen Plus software to assess gasification in fluidized bed, fixed bed and rotary kiln reactors, which are applicable for the solid waste and biomass valorization.

Other studies extensively discussed the effects of varied operating parameters, such as operating conditions, biomass feedstocks and gasifying agents, on syngas compositions. For instance, Ramzan et al. (2011) performed simulations in Aspen Plus to evaluate the gasifier performance when different biomass feedstocks were used. Watson et al. (2018) wrote a review on the biowaste gasification, in which they highlighted the advantage of using steam as a gasifying agent for enabling the production of H_2-rich syngas with high energy content gas. Cao et al. (2019) modelled the gasification process to investigate the effects of temperature, equivalence ratio and oxygen enrichment on syngas production in an oxygen-enriched air gasification system. Other discussion can be found elsewhere (Ahmad et al., 2016; Hoo et al., 2021).

While many studies widely discussed the effects of gasification operating parameters on syngas compositions, to the best of our knowledge, only fewer studies assessed and linked the effects of gasification process parameters on final products derived from syngas (Zhang et al., 2009; Yan et al., 2017; Haydary et al., 2021). Essentially, performing such evaluation gives a thorough understanding of biomass processing and provides one with useful heuristics for the conversion of biomass to valuable chemicals. Among those available in literature, Puig-Gamero et al. (2018) assessed an integrated process of biomass-to-methanol conversion, which includes gasification, syngas cleaning and methanol synthesis. However, they considered an equilibrium reactor model for the methanol synthesis and did not take into account the formation of dimethyl ether as a side product. In reality, the reaction performance is sometimes controlled by kinetics, and consequently, it affects the conversion and selectivity of the final product.

This study aims to give contribution in providing recommendations for the design of biomass-to-methanol conversion via steam gasification, in which the effects of steam-to-biomass ratio and gasifier temperature on the methanol production were simulated and assessed by considering kinetic models in the syngas-to-methanol reactions. The two parameters are discussed and assessed in the present paper as they were reported as very essential gasification process parameters in affecting the gasification performance (Puig-Arnavat et al., 2010; Shahbaz et al., 2020). The outcome of this study explicitly highlights the importance of selecting appropriate operating parameters in gasification for enhancing the production of methanol as a valuable chemical desired from the biomass processing.

RESEARCH METHODOLOGY

Materials

The biomass conversion to methanol via gasification was simulated in Aspen Plus v11. The process hierarchy of the conversion process is shown in Figure 1, in which three steps, i.e., gasification, syngas cleaning and methanol production, were included. In this study, oil palm empty fruit bunch (OPEFB) was the biomass fed to the gasification process and its ultimate and proximate analysis suggested by Mohammed et al. (2011) is presented in Table 1. OPEFB is one of the main waste products in the oil palm plantations and industries that are largely located in Southeast Asia, in which OPEFB contributes to at least one third of oil palm biomass (Geng, 2013; Pairon et al., 2022). The process simulation of the OPEFB gasification was modified from Puig-Gamero et al. (2018), while the simulation of the methanol production was adapted from Nyári et al. (2020).

A dual fluidized bed gasifier for the conversion of OPEFB to syngas was simulated in an equilibrium model, in which steam was used as a gasifying agent. The gasification process with steam was reported to be cleaner and able to deliver higher energy content than the processes with other

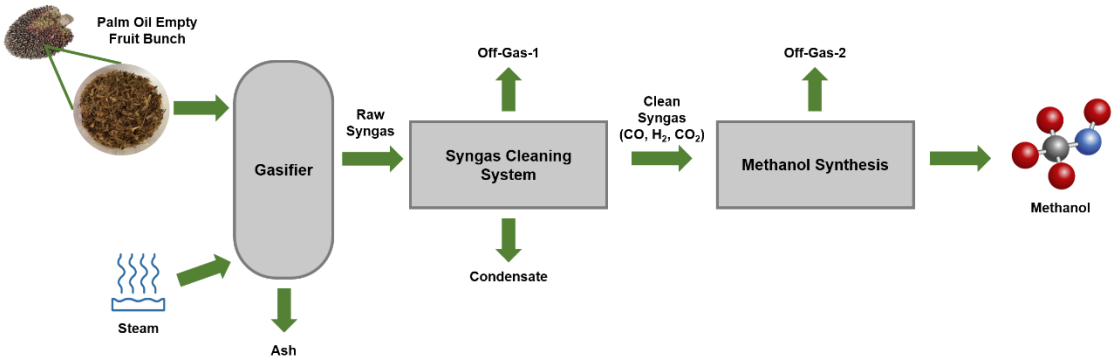

Figure 1. The conversion of OPEFB to methanol via steam gasification.

Table 1. Ultimate and proximate analysis of OPEFB (Mohammed et al., 2011).

Ultimate analysis (wt.%)					Proximate analysis (wt.%)			
C	H	N	S	O	Ash^{d}	Volatile matter^{ad}	Fixed carbon^{ad}	Moisture^{ad}
46.62	6.45	1.21	0.035	45.66	3.45	82.58	8.79	5.18

d: on dry basis, ad: on air dried basis

Table 2. Reactions in the gasification zone.

Reaction	Equation	Enthalpy	Eq.
water-gas reaction	$C + H_2O \rightleftarrows CO + H_2$	$\Delta H = 131$ kJ/mol	(1)
water-gas shift reaction	$CO + H_2O \rightleftarrows CO_2 + H_2$	$\Delta H = -41$ kJ/mol	(2)
steam reforming	$CH_4 + H_2O \rightleftarrows CO + 3H_2$	$\Delta H = 206$ kJ/mol	(3)
Boudouard reaction	$C + CO_2 \rightleftarrows 2CO$	$\Delta H = 172$ kJ/mol	(4)

agents (Watson et al., 2018; AlNouss et al., 2020). A dual fluidized bed reactor has a combustion zone that is commonly independent of the gasification zone. The air intake to the process in this study was necessary for the combustion zone, where the char combustion provided energy for the rest of the gasification process. The combustion residual came out of the process as ash. Some assumptions taken into account in the gasification process were (1) the process was steady state, (2) all gases behaved ideally, (3) char only contained carbon and ash, (4) ash was considered as an inert, (5) pressure and temperature were uniform inside the dual fluidized bed gasifier, (6) no heat losses and pressure drop occurring in the process.

The gasifier was modelled based on the Gibbs free energy minimization, with the reactions occurring in the reactor presented in Table 2. This study assessed the gasification process with the steam-to-biomass ratios (S/B) in the range of 0.3 – 0.7 and the gasifier temperatures of 900 – 1,100°C. Peng et al. (2017) suggested that a higher operating temperature in a gasifier leads to the reduction of the tar formed from the process. Moreover, Puig-Gamero et al. (2018) reported that for S/B of 0.6 the tar yields in the gasification process at 800°C and 900°C were 12.36 wt.% and $3{\cdot}10^{-3}$ wt.%, respectively. Therefore, the gasifier temperature of less than 900°C was not considered in this study. For all varied gasification conditions, the mass flow rates of biomass and steam were adjusted to achieve comparable gas superficial flow velocities in the inlet of the methanol reactor for different scenarios, i.e., within the range of 1.1 – 1.3 m/s.

The aim of gas cleaning was to remove the contaminants, i.e., H_2S and NH_3, produced during gasification. To separate clean syngas from the contaminants, pressure swing adsorption technology was simulated in this work. During the cleaning process, water was also separated and a small amount of CO and CO_2 was removed together with the contaminants.

After the removal of the contaminants, clean syngas was fed to a reactor and converted to methanol. A set of reactor configurations packed with Cu/Zn/Al/Zr catalyst proposed by Nyári et al. (2020) was used in this study as they considered a complete set of main and side reactions. The reactions involved in this process are listed in Table 3, and the reaction rates expressions and the kinetics

$$X = \frac{(F_{CO} + F_{CO_2} + F_{H_2})_{in} - (F_{CO} + F_{CO_2} + F_{H_2})_{out}}{(F_{CO} + F_{CO_2} + F_{H_2})_{in}} \times 100\% \quad (5)$$

$$S = \frac{F_{CH_3OH\,out}}{(F_{CO} + F_{CO_2} + F_{H_2})_{in} - (F_{CO} + F_{CO_2} + F_{H_2})_{out}} \times 100\% \quad (6)$$

Table 3. Reactions in the syngas conversion process to chemicals (Manenti et al., 2014).

Reaction	Equation	Enthalpy	Eq.
Carbon monoxide hydrogenation	$CO + 2H_2 \rightleftarrows CH_3OH$	$\Delta H°_{298}$ = -90.55 kJ/mol	(7)
Carbon dioxide hydrogenation	$CO_2 + 3H_2 \rightleftarrows CH_3OH + H_2O$	$\Delta H°_{298}$ = -49.43 kJ/mol	(8)
Water-gas shift	$CO_2 + H_2 \rightleftarrows CO + H_2O$	$\Delta H°_{298}$ = +41.12 kJ/mol	(9)
Methanol dehydration	$2CH_3OH \rightleftarrows CH_3OCH_3 + H_2O$	$\Delta H°_{298}$ = -23.4 kJ/mol	(10)

Table 4. Chemical reaction kinetics of the syngas conversion reactions (Nyári et al., 2020)

Kinetic Expression	Eq.
$r_A = k_A \dfrac{K_{CO}\left[f_{CO} f_{H_2}^{\frac{3}{2}} - \dfrac{f_{CH_3OH}}{f_{H_2}^{\frac{3}{2}} K_{P,A}}\right]}{\left(1 + K_{CO} f_{CO} + K_{CO_2} f_{CO_2}\right)\left[f_{H_2}^{\frac{1}{2}} + \left(\dfrac{K_{H_2O}}{K_{H_2}^{\frac{1}{2}}}\right) f_{H_2O}\right]}$	(11)
$r_B = k_B \dfrac{K_{CO_2}\left[f_{CO_2} f_{H_2} - \dfrac{f_{H_2O} f_{CO}}{K_{P,B}}\right]}{\left(1 + K_{CO} f_{CO} + K_{CO_2} f_{CO_2}\right)\left[f_{H_2}^{\frac{1}{2}} + \left(\dfrac{K_{H_2O}}{K_{H_2}^{\frac{1}{2}}}\right) f_{H_2O}\right]}$	(12)
$r_C = k_C \dfrac{K_{CO_2}\left[f_{CO_2} f_{H_2}^{\frac{3}{2}} - \dfrac{f_{CH_3OH} f_{H_2O}}{f_{H_2}^{\frac{3}{2}} K_{P,C}}\right]}{\left(1 + K_{CO} f_{CO} + K_{CO_2} f_{CO_2}\right)\left[f_{H_2}^{\frac{1}{2}} + \left(\dfrac{K_{H_2O}}{K_{H_2}^{\frac{1}{2}}}\right) f_{H_2O}\right]}$	(13)
$r_D = k_D \dfrac{K_{CH_3OH}^2\left[C_{CH_3OH}^2 - \dfrac{\left(C_{H_2O} C_{DME}\right)}{K_{P,D}}\right]}{\left(1 + 2\sqrt{K_{CH_3OH} C_{CH_3OH}} + K_{H_2O} C_{H_2O}\right)^4}$	(14)

r_A, r_B, r_C and r_D are the reaction rates for carbon monoxide hydrogenation, carbon dioxide hydrogenation, water-gas shift and methanol dehydration, respectively. k_A, k_B, k_C and k_D are their corresponding reaction rate constants for each reaction rate.

parameters are shown in Table 4 and Table 5. In this study, the amount of CO, H_2 and CO_2 entering the methanol reactor was dependent on S/B and gasifier temperatures that were previously varied. The conversion and selectivity of reactions occurring in the reactor will be discussed in the next section. The conversion of the set of reactions is defined as the difference of total mass flow rates of CO, CO_2 and H_2 entering the reactor and total mass flow rates of CO, CO_2 and H_2 leaving the reactor divided by total mass flow rates of CO, CO_2 and H_2 entering the reactor as shown in Eq. (5).

The selectivity of the set of reactions to methanol is defined as the mass flow rate of CH_3OH leaving the reactor divided by the converted CO, CO_2 and H_2 in the reactor, as shown in Eq. (6).

Table 5. Kinetics parameters of the syngas conversion reactions (Kiss et al., 2016; Nyári et al., 2020)

Parameter	Value	Unit	Eq.
k_A	$4.0638 \times 10^{-6} \exp\left(-\frac{11695}{\mathrm{RT}}\right)$	kmol/kg_{cat} s Pa	(15)
k_B	$9.0421 \times 10^{8} \exp\left(-\frac{112860}{\mathrm{RT}}\right)$	kmol/kg_{cat} s $Pa^{0,5}$	(16)
k_C	$1.5188 \times 10^{-33} \exp\left(-\frac{266010}{\mathrm{RT}}\right)$	kmol/kg_{cat} s Pa	(17)
k_D	$8.54 \times 10^{6} \exp\left(-\frac{123779}{\mathrm{RT}}\right)$	kmol/kg_{cat} s Pa	(18)
K_{CO}	$8.3965 \times 10^{-11} \exp\left(\frac{118270}{\mathrm{RT}}\right)$	Pa^{-1}	(19)
K_{CO_2}	$1.7214 \times 10^{-10} \exp\left(\frac{81287}{RT}\right)$	Pa^{-1}	(20)
$K_{H_2O}/K_{H_2}^{0,5}$	$4.3676 \times 10^{-12} \exp\left(\frac{115080}{RT}\right)$	$Pa^{-0,5}$	(21)
K_{CH_3OH}	$7.9 \times 10^{-4} \exp\left(\frac{70500}{RT}\right)$	m^3/kmol	(22)
$K_{P,A}$	$2.31 \times 10^{-23} \exp\left(\frac{98438}{RT}\right)$	Pa^{-2}	(23)
$K_{P,B}$	$2.81 \times 10^{-2} \exp\left(\frac{43939}{RT}\right)$	-	(24)
$K_{P,C}$	$6.5 \times 10^{-21} \exp\left(\frac{54499}{RT}\right)$	Pa^{-2}	(25)
$K_{P,D}$	$1.06 \times 10^{-1} \exp\left(\frac{21858}{RT}\right)$	-	(26)

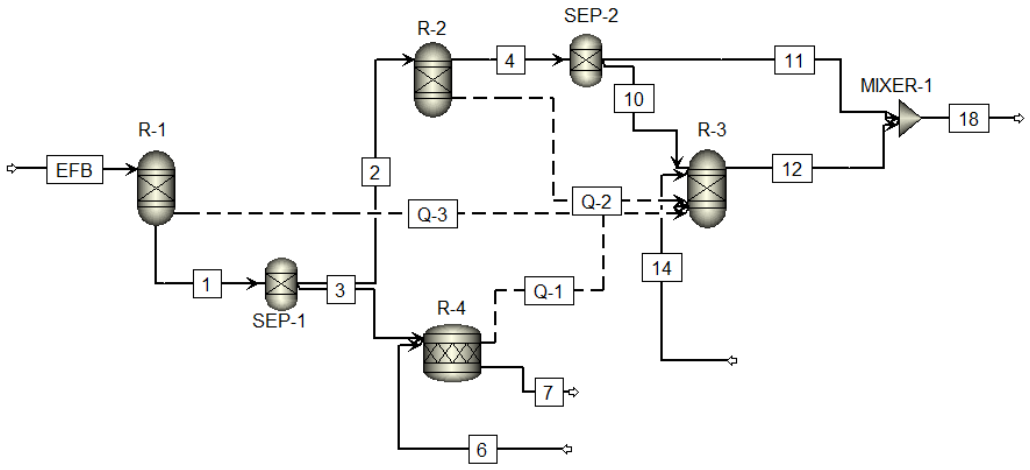

Figure 2. Process flowsheet of oil palm empty fruit bunch gasification

RESULTS AND DISCUSSION

The process flowsheet of the oil palm empty fruit bunch gasification obtained from simulation is presented Figure 2. Before the biomass stream entered the gasifier (R-3, a Gibbs reactor), OPEFB initially came into a process unit for simultaneous drying and pyrolysis (R-1, a yield reactor), where the biomass was broken down into its constituent components and ash. The components leaving the unit have mass compositions according to the ultimate and proximate analysis of the biomass. Char was split by using SEP-1 and it entered a combustion zone (R-4, a stoichiometric reactor). As the operating conditions in both combustion and gasification zones were equal, the amount of char split by using SEP-1 was computed via a design specification

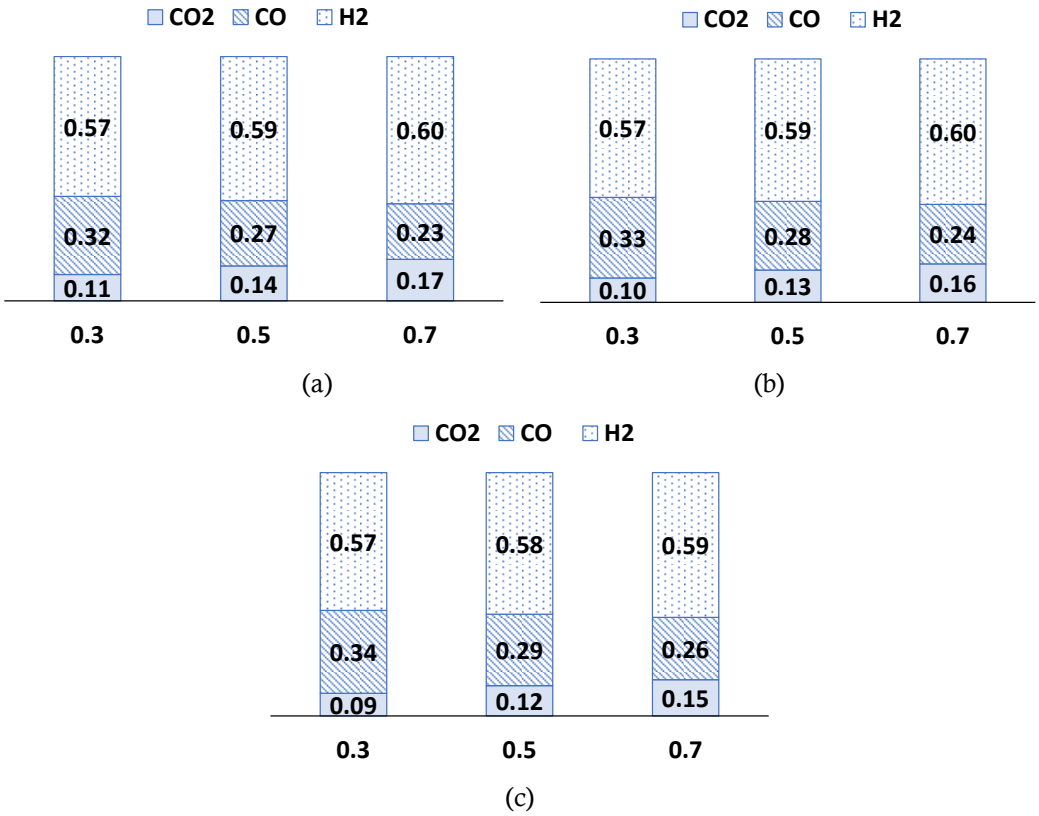

Figure 3. Effect of steam-to-biomass ratio on the mol fractions of the gasification products for the operating temperatures of (a) 900°C, (b) 1,000°C and (c) 1,100°C.

block in order to achieve a uniform targeted temperature in both zones. The air intake to the combustion zone was calculated using a design specification by considering an air excess of 1.2 relative to char being combusted (Puig-Gamero et al., 2018). The drying and pyrolysis products were then sent to R-2 (an equilibrium reactor) to fix the main products as C, H_2, CO_2, CO, CH_4, H_2S and NH_3. The R-2 outlet was fed to SEP-2 to separate H_2S and NH_3. Then, other components were introduced to the gasification zone (R-3, a Gibbs reactor) with the required energy being supplied from the combustion section.

The mol fractions of the gasification products are depicted in Figure 3. For each S/B ratio and a specified gasification temperature, produced CH_4 was very low, i.e., less than 0.1 mol%; therefore, it is not shown in Figure 3. For a fixed temperature, the higher S/B ratio enabled the total consumption of carbon in the water-gas reaction (Eq. (1)), which produced CO and H_2. The higher amount of H_2O then pushed the water-gas shift reaction (Eq. (2)) to the products side. Therefore, one can notice the reduced amount of CO and the increase production of CO_2 and H_2 for a higher S/B ratio. The finding of the reduced CO and increased H_2 amounts for a higher S/B ratio is consistent with that suggested Al-Zareer et al. (2016), in which they assessed the syngas quality produced from various types of coal and different steam flow rates to the gasifier. While, for a fixed S/B ratio, the rise of the gasification temperature leads to the slight increase of CO, the small decrease of CO_2 and the negligible change of H_2. These trends can be explained by the Le Chatelier's principle, in which the equilibrium shifts toward products when the temperature of an endothermic reaction is increased; and the reverse effect can be observed for an exothermic reaction. As the water-gas reaction (Eq. (1)) is an endothermic reaction, more CO was produced when the temperature was higher. While, because the water-gas shift reaction (Eq. (2)) is an exothermic reaction, less CO_2 was obtained with the rise of the gasification temperature. The negligible change in the H_2 mol fraction is due to a trade-off between its higher production in the water-gas reaction (Eq. (1)) and its lower production in the water-gas shift reaction (Eq. (2)).

Compared to varied S/B ratios, the modified gasifier temperatures relatively gave smaller changes to the gases mol fractions. For

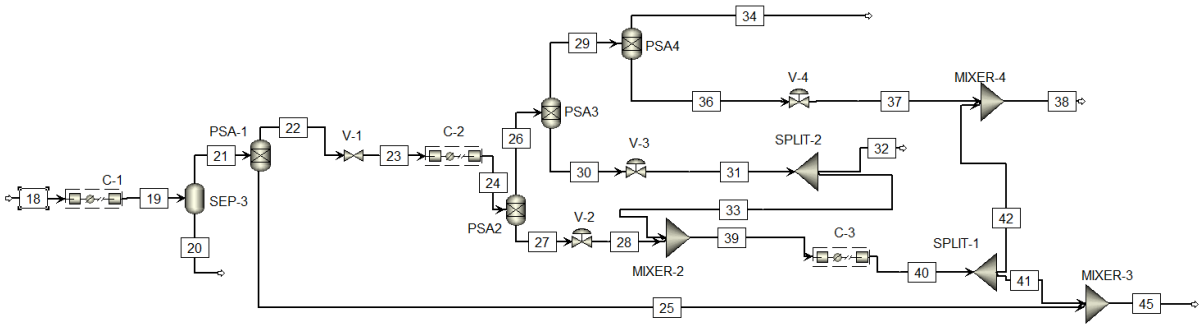

Figure 4. Process flowsheet of syngas cleaning

Table 6. Split fraction in the pressure swing adsorption system (Gutiérrez et al., 2017)

Component	PSA-1 (top)	PSA-2 (bottom)	PSA-3 (top)	PSA-4 (top)
	H_2-rich stream	CO-rich stream	CH_4-rich stream	CH_4-rich stream
H_2	95	-	4.5	-
CO	-	98	1.5	-
CO_2	-	1	9	-
CH_4	-	1	90	100

instance, for S/B = 0.3 and varied gasifier temperatures, the mol fractions of CO vary from 0.32 to 0.34 (the absolute difference is 0.02). While, for the gasifier temperature of 900°C and varied S/B ratios, the mol fractions of CO vary from 0.23 to 0.32 (the absolute difference is 0.09). The same trends can be observed for other gasification products. Based on the results, it can be observed that the gasification products distribution is more sensitive to the change of the S/B ratio than to the modification of the gasification temperature.

The raw syngas generated from the gasification unit was then introduced to the syngas cleaning unit, in which the pressure swing adsorption (PSA) was applied to remove unwanted compounds, i.e., NH_3, H_2S, CH_4 and H_2O. The PSA process was modeled by four separator blocks operating at 35°C and 30 atm. The mol percentages of recovered compounds were obtained from Gutiérrez et al. (2013) and listed in Table 6. The depressurization process was simulated by using a valve for each of the PSA off-gas streams. Before entering the PSA system, initially syngas was compressed to 30 atm and cooled down to 35°C by applying a multistage compressor (C-1). Then, the condensed water was separated from the gas stream by SEP-4. The use of the first PSA unit (PSA-1) was aimed to recover H_2 from the syngas stream. The top stream of PSA-2 was introduced to the second PSA unit (PSA-2), where the separation of CO_2 occurred. The top outlet of PSA-2 entered the third PSA unit (PSA-3) for further gases split where CH_4 left to the top (stream 29) and CO_2 left to the bottom (stream 30). The CH_4-rich top then entered the fourth PSA unit (PSA-4) and CH_4 was separated (stream 34) from other gases. The H_2-rich stream from the PSA-1 (stream 25) was mixed with the mixture of CO and CO_2 coming out from the rest of PSA's off-gas streams (stream 41) before further entering the syngas conversion unit. The mol fractions of clean syngas sent to the syngas conversion unit are presented in Table 7. These different mol fractions were obtained as the consequence of applying varied S/B ratios and operating temperatures in the gasification process. The process flowsheet of syngas cleaning unit can be seen in Figure 4.

The pure syngas was fed into a methanol synthesis unit with the reactor configurations proposed by Nyári et al. (2020). For the reproducibility check (Table 8), exact reactor inlet conditions and compositions as those used by Nyári et al. (2020) were initially applied to the simulation in this work. Then, syngas with different mol fractions as shown in Table 7 was fed to the reactor.

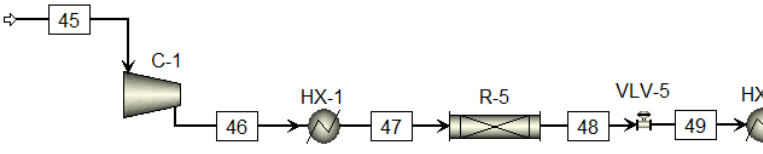

Figure 5 demonstrates the process flowsheet of the syngas conversion to methanol. At

first, syngas was compressed to 50 bar and heated up to a temperature of 230°C before being introduced to an isothermal plug-flow reactor packed with the commercial Cu/Zn/Al/Zr catalysts. The product stream exiting from the reactor was depressurized to 1 atm, cooled down to

Table 7. Mol fractions of gases after syngas cleaning

S/B	Mol fraction								
	T_{gasif} = 900°C			T_{gasif} = 1,000°C			T_{gasif} = 1,100°C		
	CO_2	CO	H_2	CO_2	CO	H_2	CO_2	CO	H_2
0.3	0.004	0.364	0.632	0.004	0.374	0.622	0.004	0.380	0.616
0.5	0.006	0.317	0.677	0.006	0.330	0.664	0.005	0.340	0.655
0.7	0.007	0.278	0.714	0.007	0.294	0.699	0.006	0.306	0.688

Table 8. Reproducibility of reactor configurations proposed by Nyári et al. (2020)

	Reactor inlet*	Reactor outlet (Nyári et al. (2020))	Reactor outlet (simulation result in this work)
Temperature (°C)	230	230	230
Pressure (bar)	50	49.7	49.7
Mass vapor fraction	1	1	1
Total mol flow rate (kmol/h)	$1.64 \cdot 10^5$	$1.51 \cdot 10^5$	$1.50 \cdot 10^5$
Total mass flow rate (kg/h)	$9.17 \cdot 10^5$	$9.17 \cdot 10^5$	$9.17 \cdot 10^5$
Mass fraction			
H_2O	0.00135	0.130	0.138
CH_3OH	0.0131	0.242	0.257983
H_2	0.328	0.285	0.281975
CO_2	0.623	0.308	0.290598
CO	0.0295	0.0295	0.02714
O_2	0.000	0.000	0
N_2	0.000	0.000	0
CH_3OCH_3	0.0047	0.0048	0.004721

*The reactor inlet simulated in this work for the reproducibility check was set identical to that proposed by Nyári et al. (2020).

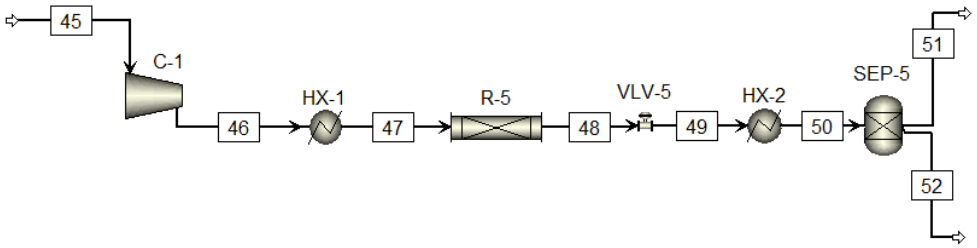

Figure 5. Process flowsheet of syngas conversion to methanol.

30°C and separated into crude methanol and non-reacted gases.

The syngas conversion (X) and the reaction selectivity to methanol (S) were calculated using Eq. (5) and (6), and those numbers are depicted in Figure 6. For a fixed temperature (Figure 6 (a)), the increase of S/B ratio from 0.3 to 0.7 allows the syngas conversion to jump by 18% – 19%. For instance, at 900°C, the syngas conversions rise from 60.7% to 71.7%. While, for a constant S/B ratio, the rise of temperature from 900°C to 1,100°C causes the conversion reduction by 3% – 5%. For example, for S/B = 0.5, the conversion decreases from 67.9% to 64.6%. These changes indicate that the syngas conversion is more affected by the steam-to-biomass ratio than the gasification temperature.

While the sensitivity of the syngas conversion is observed, the reaction selectivity to methanol remains high and unchanged (>99.9%) with the varied S/B ratios and gasifier temperatures, as shown in Figure 6 (b). This result indicates that the reaction pathways toward methanol (Eq. (7) and (8)) are very much favored than that toward dimethyl ether as a side product.

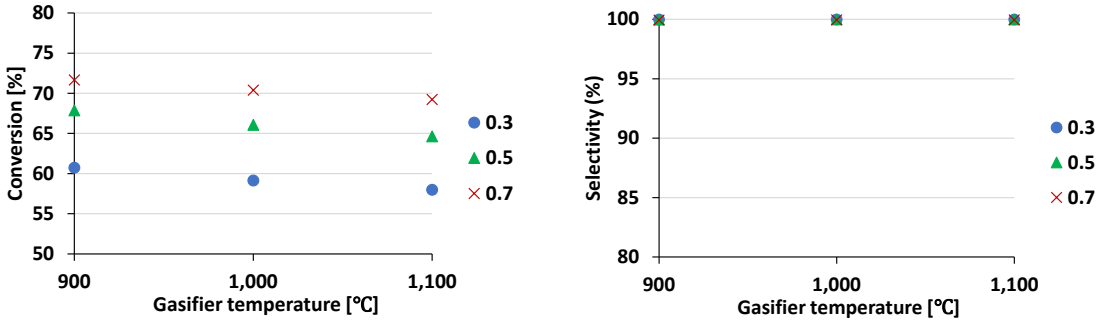

(a) (b)

Figure 6. (a) Syngas conversion and (b) reaction selectivity to methanol at varied S/B ratios and gasifier temperatures.

CONCLUSION

This study evaluated varied steam-to-biomass ratios and gasification temperatures for the biomass-to-methanol conversion via steam gasification. A better understanding of their effects on the methanol production has been gained. The rise of the steam-to-biomass ratio reduces CO and increases CO_2 and H_2 in the gasification distribution products. While, the increase of the gasification temperature brings an opposite effect on the CO and CO_2 amounts. It is concluded that the distribution of gasification products is more sensitive to the change of the S/B ratio than to the modification of the gasification temperature.

The change of the syngas-to-methanol conversion was observed when steam-to-biomass ratios and gasification temperatures were varied. The increase of the syngas conversion can be obtained by applying a higher steam-to-biomass ratio and operating the gasifier at a sufficiently high temperature, i.e., at 900°C. Note that selecting lower temperature potentially causes the tar formation, as suggested by Puig-Gamero et al. (2018). Similar to the distribution of gasification products, the syngas conversion was found to be more sensitive to the change of S/B ratio than to the varied gasification temperature. While, the reaction selectivity to methanol remains unaffected when steam-to-biomass ratios and gasification temperatures were varied. As the results of the sensitivity analysis conducted in this study for the steam-to-biomass ratios (S/B) in the range of 0.3 – 0.7 and the gasifier temperatures of 900 – 1,100°C, the optimum process performance was achieved when S/B and the gasifier temperature are 0.7 and 900°C, respectively.

LIST OF NOTATIONS

C_i	molarity of compound i
F_i	mass flow rate of compound i
f_i	fugacity of compound i
k_i	reaction rate constant for reaction i
K_i	adsorption equilibrium constant for compound i
$K_{P,i}$	equilibrium constant of reaction i
R	ideal gas constant
r_i	reaction rate for compound i
S	selectivity
T_{gasif}	gasification temperature
X	conversion

REFERENCES

Abdelouahed, L., Authier, O., Mauviel, G., Corriou, J.P., Verdier, G., Dufour, A. 2012. Detailed Modeling of Biomass Gasification in Dual Fluidized Bed Reactors under Aspen Plus. Energy & Fuels. 26(6): 3840–3855.

Ahmad, A.A., Zawawi, N.A., Kasim, F.H., Inayat, A., Khasri, A. 2016. Assessing the gasification performance of biomass: A review on biomass gasification process conditions, optimization and economic evaluation. Renewable and Sustainable Energy Reviews. 53: 1333–1347.

AlNouss, A., McKay, G., Al-Ansari, T. 2020. A comparison of steam and oxygen fed biomass gasification through a techno-economic-environmental study. Energy Conversion and Management. 208: 112612.

Al-Zareer, M., Dincer, I., Rosen, M.A. 2016. Effects of various gasification parameters and operating conditions on syngas and hydrogen production. Chemical Engineering Research and Design. 115: 1–18.

Begum, S., Rasul, M.G., Akbar, D., Cork, D. 2014. An Experimental and Numerical Investigation of Fluidized Bed Gasification of Solid Waste. Energies. 7: 43–61.

Cao, Y., Wang, Q., Du, J., Chen, J. 2019. Oxygen-enriched air gasification of biomass materials for high-quality syngas production. Energy Conversion and Management. 199: 111628.

Fajimi, L. I., Oboirien, B. O., Adams II, T. A. 2021. Simulation studies on the co-production of syngas and activated carbon from waste tyre gasification using different reactor configurations. Energy Conversion and Management: X. 11: 100105.

Gao, X., Zhang, Y., Li, B., Yu, X. 2016. Model development for biomass gasification in an entrained flow gasifier using intrinsic reaction rate submodel. Energy Conversion and Management. 108: 120–131.

Geng, A. 2013. Conversion of oil palm empty fruit bunch to biofuels. Liquid, Gaseous and Solid Biofuels-Conversion Techniques. InTech. Croatia.

Gutiérrez Ortiz, F.J., Serrera, A., Galera, S., Ollero, P. 2013. Methanol synthesis from syngas obtained by supercritical water reforming of glycerol. Fuel. 105: 739–751.

Haydary, J., Šuhaj, P., Husár, J. 2021. Waste biomass to methanol – optimization of gasification agent to feed ratio. Biomass Conversion and Biorefinery. 11: 419–428.

Hoo, K.K., Md Said, M.S. 2021. Air gasification of empty fruit bunch: An Aspen Plus model. Bioresource Technology Reports. 16: 100848.

Kiss, A.A., Pragt, J.J., Vos, H.J., Bargeman, G., de Groot, M.T. 2016. Novel efficient process for methanol synthesis by CO_2 hydrogenation. Chemical Engineering Journal. 284: 260–269.

Manenti, F., Leon-Garzon, A.R., Ravaghi-Ardebili, Z., Pirola, C. 2014. Systematic staging design applied to the fixed-bed reactor series for methanol and one-step methanol/dimethyl ether synthesis. Applied Thermal Engineering. 70(2): 1228–1237.

Marulanda, V.A., Gutierrez, C.D.B., Alzate, C.A.C. 2019. Chapter 4 Thermochemical, Biological, Biochemical, and Hybrid Conversion Methods of Bio-derived Molecules into Renewable Fuels, in M. Hosseini (Ed.) Advanced Bioprocessing for Alternative Fuels, Biobased Chemicals, and Bioproducts. Woodhead Publishing. 59–81.

Mohammed, M.A.A., Salmiaton, A., Wan Azlina, W.A.K.G., Mohammad Amran, M.S., Fakhru'l-Razi, A. 2011. Air gasification of empty fruit bunch for hydrogen-rich gas production in a fluidized-bed reactor. Energy Conversion and Management. 52(2): 1555–1561.

Molino, A., Larocca, V., Chianese, S., Musmarra, D. 2018. Biofuels Production by Biomass Gasification: A Review. Energies. 11(4): 811.

Mutlu, Ö.Ç., Zeng, T. 2020. Challenges and Opportunities of Modeling Biomass Gasification in Aspen Plus: A Review. Chemical Engineering & Technology. 43(9): 1674–1689.

Nyári, J., Magdeldin, M., Larmi, M., Järvinen, M., Santasalo-Aarnio, A. 2020. Techno-economic barriers of an industrial-scale methanol CCU-plant. Journal of CO_2 Utilization. 39: 101166.

Pairon, M.S., Ali, F., Ahmad, F., Anuar, H., Abdul Rahman, N.A., Saeed Mirghani, M.E., Suhr, J., Thomas, S. 2022. Review on Solvent Extraction Methods of Lignin from Oil Palm Empty Fruit Bunches (OPEFB). Journal of Natural Fibers. 19(15): 11507–11523.

Panwar, N.L., Kothari, R., Tyagi, V.V. 2012. Thermo chemical conversion of biomass – Eco friendly energy routes. Renewable and Sustainable Energy Reviews. 16(4): 1801–1816.

Peng, W.X., Wang, L.S., Mirzaee, M., Ahmadi, H., Esfahani, M.J., Fremaux, S. 2017. Hydrogen and syngas production by catalytic biomass gasification. Energy Conversion and Management. 135: 270–273.

Puig-Arnavat, M., Bruno, J.C., Coronas, A. 2010. Review and analysis of biomass gasification models. Renewable and Sustainable Energy Reviews. 14: 2841–2851.

Puig-Gamero, M., Argudo-Santamaria, J., Valverde, J.L., Sánchez, P., Sanchez-Silva, L. 2018. Three integrated process simulation using aspen plus®: Pine gasification, syngas cleaning and methanol synthesis. Energy Conversion and Management. 177: 416–427.

Ramzan, N., Ashraf, A., Naveed, S., Malik, A. 2011. Simulation of hybrid biomass gasification using Aspen plus: A comparative performance analysis for food, municipal solid and poultry waste. Biomass and Bioenergy. 35(9): 3962–3969.

Shahbaz, M., Al-Ansari, T., Inayat, M., Sulaiman, S.A., Parthasarathy, P., McKay, G. 2020. A critical review on the influence of process parameters in catalytic co-gasification: Current performance and challenges for a future prospectus. Renewable and Sustainable Energy Reviews. 134: 110382.

Vu, H. P., Nguyen, L. N., Vu, M. T., Johir, M. A. H., McLaughlan R., Nghiem, L. D. 2020. A comprehensive review on the framework to valorise lignocellulosic biomass as biorefinery feedstocks. Science of the Total Environment. 743: 140630.

Xiong, X., Yu, I.K.M., Cao, L., Tsang, D.C.W., Zhang, S., Ok, Y.S. 2017. A review of biochar-based catalysts for chemical synthesis, biofuel production, and pollution control. Bioresource Technology. 246: 254–270.

Watson, J., Zhang, Y., Si, B., Chen, W.-T., de Souza, R. 2018. Gasification of biowaste: A critical review and outlooks. Renewable and Sustainable Energy Reviews. 83: 1–17.

Yan, L., Li, Y., Li, J., Gao, W. 2017. Steam gasification of biomass for biomethanol production: Model development and analysis. Energy Sources, Part A: Recovery, Utilization, and Environmental Effects. 39(13): 1410–1415.

You, S., Ok, Y.S., Tsang, D.C.W., Kwon, E.E., Wang, C.-H. 2018. Towards practical application of gasification: a critical review from syngas and biochar perspectives. Critical Reviews in Environmental Science and Technology. 48(22-24): 1165–1213.

Zhang, Y., Xiao, J., Shen, L. 2009. Simulation of methanol production from biomass gasification in interconnected fluidized beds. Industrial & Engineering Chemistry Research. 48(11): 5351–5359.

Zhang, L., Xu, C., Champagne, P. 2010. Overview of recent advances in thermo-chemical conversion of biomass. Energy Conversion and Management. 51(5): 969–982.